Letter

Resolving the spurious-state problem in the Dirac equation with the finite-difference method

Ying Zhang
Department of Physics, School of Science, Tianjin University, Tianjin 300354, China

Yuxuan Bao and Hong Shen*
School of Physics, Nankai University, Tianjin 300071, China

Jinniu Hu†
School of Physics, Nankai University, Tianjin 300071, China
and Shenzhen Research Institute of Nankai University, Shenzhen 518083, China

(Received 22 July 2022; revised 1 November 2022; accepted 8 November 2022; published 18 November 2022)

To solve the Dirac equation with the finite-difference method, one has to face the spurious-state problem due to the fermion doubling problem when using the conventional central difference formula to calculate the first-order derivative on equal interval lattices. This problem is resolved by replacing the central difference formula with the asymmetric difference formula, i.e., the backward or forward difference formula. To guarantee the hermiticity of the Hamiltonian matrix, the backward and forward difference formula should be used alternatively according to the parity of the wave function. This provides a simple and efficient numerical prescription to solve various relativistic problems in the microscopic world.

DOI: 10.1103/PhysRevC.106.L051303

The Dirac equation is essential to describe relativistic systems consisting of spin-$\frac{1}{2}$ particles in atomic physics, nuclear physics, and particle physics. The Dirac equation is a coupled first-order differential equation for wave functions with large and small components. It can be solved analytically with very few potentials. Therefore, the numerical methods to obtain the eigenenergies and wave functions of the Dirac equation are highly demanded in the relevant fields. Many numerical technologies have been applied to solve the Dirac equation, such as the shooting method [1,2], basis expansion method [3–6], finite-difference method (FDM) [7–9], finite-element method (FEM) [10–15], Green's function method [16], imaginary time step (ITS) method [17], inverse Hamiltonian method [18,19], conjugate gradient method [20], and so on. Among these methods, the shooting and basis expansion methods are quite robust. They are extensively used to solve the Dirac equation in the relativistic mean-field model, which is a powerful tool to describe many nuclear properties [2,21–24]. However, these two methods are very sensitive to the box size or basis space for the weakly bound states. The Green's function method is not sensitive to the space size but cannot give the eigenenergies and wave functions directly. The ITS, inverse Hamiltonian, and conjugate gradient methods are also friendly to the space size but they need steps of evolutions to achieve the final solutions.

The FDM is a very simple and efficient method to solve the differential equation, where the derivative operator is easily replaced by a combination of several function values with the finite-difference formula. This method does not need any evolution process. It achieves great success in solving the Schrödinger equation [25]. In the lattice quantum chromodynamics (LQCD) theory [26,27], researchers found a so-called "fermion doubling" problem when the Dirac field is discretized with a central difference formula (CDF), i.e., more fermionic states than expected were obtained. On the other hand, one could get spurious solutions with rapidly oscillating wave functions mixing with the physical solutions in solving the Dirac equation with FDM for the same reason.

LQCD atttempts to remove the fermion doubling problem by introducing an external energy term in the Hamiltonian, i.e., the Wilson term, which modifies the energy-momentum dispersion relation of Dirac particle and shifts the spurious state to the continuum spectrum [28,29]. Alternatively, the high-accurate finite-difference formula for the first-order derivative with more lattice points can also help to reduce the number of spurious states in Dirac equation [7,8].

In this work, we will propose a novel and simple prescription to solve the spurious-state problem when solving the Dirac equation with the FDM for massive fermions without adding any artificial terms. For a numerical illustration, we will take the nucleons of a finite nucleus moving in a Dirac Woods-Saxon potential as an example to explain this prescription.

The Dirac equation describing a nucleon with the mass M moving in the scalar $S(\boldsymbol{r})$ and vector $V(\boldsymbol{r})$ potentials can be written as [2]

$$\{\boldsymbol{\alpha}\cdot\boldsymbol{p}+V(\boldsymbol{r})+\boldsymbol{\beta}[M+S(\boldsymbol{r})]\}\Psi(\boldsymbol{r})=\varepsilon\Psi(\boldsymbol{r}), \tag{1}$$

*songtc@nankai.edu.cn
†hujinniu@nankai.edu.cn

TABLE I. The neutron energy levels of ^{132}Sn for $\kappa = -1$ and $\kappa = 1$ in the Woods-Saxon potential obtained by the FDM with different difference formulas and shooting method. The spurious states are marked in boxes. The unit of the energy level is MeV.

3PCDF		5PCDF		3PADF		5PADF		Shooting	
$\kappa=-1$	$\kappa=1$	$\kappa=-1$	$\kappa=1$	$\kappa=-1$	$\kappa=1$	$\kappa=-1$	$\kappa=1$	$\kappa=-1$	$\kappa=1$
−55.006	[−55.006]	−55.005	[−51.734]	−55.004	−46.157	−55.005	−46.162	−55.005	−46.162
[−46.165]	−46.165	[−35.186]	−46.162	−33.915	−21.377	−33.929	−21.405	−33.929	−21.405
−33.937	[−33.937]	−33.930	−21.405	−9.171	−0.284	−9.210	−0.304	−9.210	−0.259
[−21.419]	−21.419	−9.211	[−14.263]						
−9.230	[−9.230]	−0.290							

where $\boldsymbol{\alpha}$ and $\boldsymbol{\beta}$ are the Dirac matrices, and ε and $\Psi(\boldsymbol{r})$ are the eigenenergy and the corresponding wave function, respectively.

In a spherical system, the wave function can be written as

$$\Psi(\boldsymbol{r}) = \frac{1}{r}\begin{pmatrix} G(r)Y_{ljm} \\ iF(r)Y_{\tilde{l}jm} \end{pmatrix}, \tag{2}$$

where $l = j \pm 1/2$ and $\tilde{l} = 2j - l$. $G(r)$ and $F(r)$ are the large and small components of the wave function, respectively. $Y_{ljm}(\hat{\boldsymbol{r}})$ is the spin spherical harmonics. Therefore, the radial Dirac equation can be obtained as

$$\begin{pmatrix} \Sigma(r) & \frac{\kappa}{r} - \frac{d}{dr} \\ \frac{\kappa}{r} + \frac{d}{dr} & \Delta(r) \end{pmatrix}\begin{pmatrix} G(r) \\ F(r) \end{pmatrix} = E\begin{pmatrix} G(r) \\ F(r) \end{pmatrix}, \tag{3}$$

where

$$\begin{aligned} \Sigma(r) &= V(r) + S(r), \\ \Delta(r) &= V(r) - S(r) - 2M, \\ E &= \varepsilon - M, \\ \kappa &= (-1)^{j+l+1/2}(j+1/2). \end{aligned} \tag{4}$$

We take the Woods-Saxon potentials describing the finite nuclei for the $\Sigma(r)$ and $\Delta(r)$ fields from the relativistic mean-field model. The details can be found in Ref. [30]. Explicitly, we take the neutron in the nucleus ^{132}Sn $(N = 82,\ Z = 50)$ as an example in the following calculation.

With the FDM, the first-order derivative operator d/dr in Eq. (3) can be replaced by a numerical differentiation formula on the equal interval lattices. Then the Dirac Hamiltonian in Eq. (3) can be expressed as a matrix in the coordinate space. The eigenenergies and wave functions can be easily obtained by diagonalizing this Dirac Hamiltonian matrix.

There are many formulas for the finite-difference approximations to calculate the first-order derivative. The three-point CDF is the simplest one that approximates the first-order derivative of a function $f(r)$ at r by

$$\frac{df(r)}{dr} \simeq \frac{f(r+h) - f(r-h)}{2h}, \tag{5}$$

where h is the lattice interval. If the position r is equally discretized as n lattices, the first-order derivative of $f(r)$ can be written in a matrix form,

$$\frac{d}{dr} = \frac{1}{2h}\begin{pmatrix} 0 & 1 & & & & \\ -1 & 0 & 1 & & & \\ & & \ddots & & & \\ & & & -1 & 0 & 1 \\ & & & & -1 & 0 \end{pmatrix}. \tag{6}$$

In the following calculation, we take a box with $R_{\text{box}} = 20$ fm and $n = 500$ lattices. Furthermore, we assume the boundary condition for the wave functions as $f(r) = 0$ for $r = 0$ and outside the box, $r > R_{\text{box}}$. Then, the Dirac equation (3) can be written in the matrix form as

$$\left(\begin{array}{c|c} \boldsymbol{A} & \boldsymbol{B_1} \\ \hline \boldsymbol{B_2} & \boldsymbol{C} \end{array}\right)\begin{pmatrix} \boldsymbol{G} \\ \boldsymbol{F} \end{pmatrix} = E\begin{pmatrix} \boldsymbol{G} \\ \boldsymbol{F} \end{pmatrix}, \tag{7}$$

where $\boldsymbol{G}$ is a vector for the large component of wave function, $G(r)$ at $r_1 = h,\ r_2 = 2h, \ldots,\ r_{n-1} = (n-1)h,\ r_n = nh$,

$$\boldsymbol{G} = \begin{pmatrix} G(r_1) \\ G(r_2) \\ \vdots \\ G(r_{n-1}) \\ G(r_n) \end{pmatrix}, \tag{8}$$

and $\boldsymbol{F}$ has a structure similar to $\boldsymbol{G}$ but for the small component. The matrices $\boldsymbol{A}$ and $\boldsymbol{C}$ are diagonal with $\Sigma(r)$ and $\Delta(r)$. The matrix $\boldsymbol{B}_1$ can be written as

$$\boldsymbol{B}_{1c} = \begin{pmatrix} \frac{\kappa}{r_1} & -\frac{1}{2h} & & & & \\ \frac{1}{2h} & \frac{\kappa}{r_2} & -\frac{1}{2h} & & & \\ & & \ddots & & & \\ & & & \frac{1}{2h} & \frac{\kappa}{r_{n-1}} & -\frac{1}{2h} \\ & & & & \frac{1}{2h} & \frac{\kappa}{r_n} \end{pmatrix}, \tag{9}$$

and $\boldsymbol{B}_{2c} = \boldsymbol{B}_{1c}^T$.

After diagonalizing the above Dirac Hamiltonian matrix (7), one can get n sets of eigenenergies and the corresponding wave functions. The first five bound states obtained by the above FDM using the three-point CDF (3PCDF) for the states $ns_{1/2}$ $(\kappa = -1)$ and $np_{1/2}$ $(\kappa = 1)$ are shown in the columns 3PCDF in Table I. For comparison, the results obtained by the shooting method are also listed in the same table. One can find pairs of degenerate solutions between $\kappa = 1$ and $\kappa = -1$. The

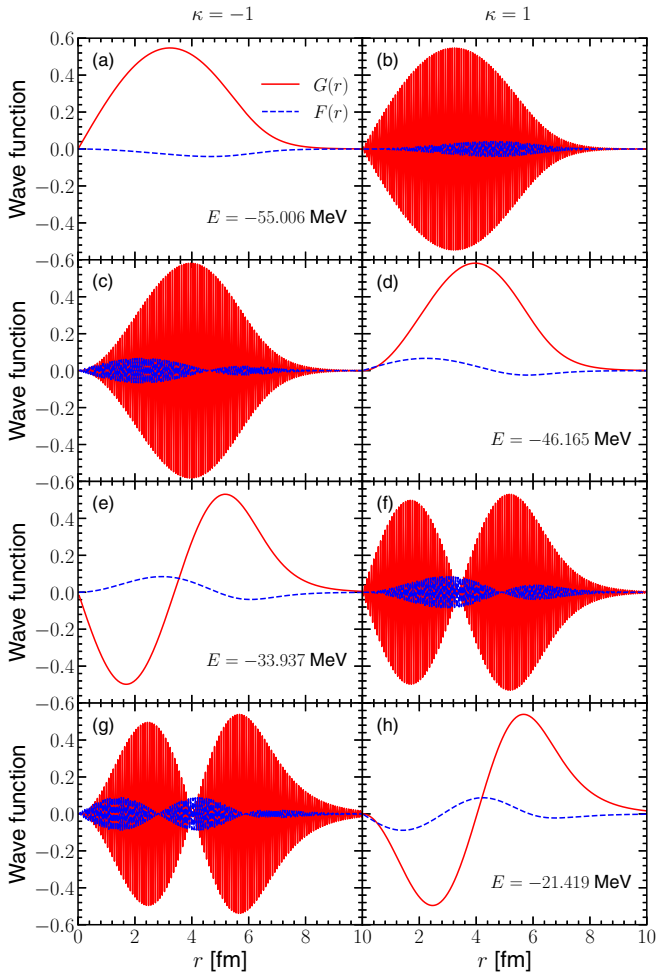

FIG. 1. The wave functions of neutrons in ^{132}Sn for the states with $\kappa = -1$ and $\kappa = 1$ in Woods-Saxon potential obtained by the FDM with three-point CDF.

large and small components of their wave functions are shown in Fig. 1. The panels (a) and (b) of Fig. 1 show the wave functions of the states with the same energy $E = -55.006$ MeV obtained for $\kappa = -1$ and $\kappa = 1$, respectively. It is easy to identify the physical state $1s_{1/2}$ in panel (a) for $\kappa = -1$, but the spurious state with rapidly oscillating wave functions is observed in panel (b) for $\kappa = 1$. Similar spurious states appear in panels (c), (f), and (g) for the states with energies $E = -46.165$ MeV ($\kappa = -1$), $E = -33.937$ MeV ($\kappa = 1$), and $E = -21.419$ MeV ($\kappa = -1$), respectively. All the spurious states are marked in boxes in Table I. On the other hand, the physical solutions have energies close to those obtained by the shooting method.

Actually, the origin of the above degenerate physical and spurious states was demonstrated in Ref. [9]. Zhao found that if the first-order derivative is calculated by the three-point CDF as in Eq. (6), there exists a unitary matrix U that transforms the Hamiltonian with κ, H_κ to that with $-\kappa$, $H_{-\kappa}$, i.e., $UH_\kappa U^{-1} = H_{-\kappa}$. This matrix U has alternating ± 1 diagonal elements. As a result, one can obtain the degenerate energy solutions $E_\kappa = E_{-\kappa}$, with the wave functions $\phi_\kappa = U\phi_{-\kappa}$. If the wave function $\phi_{-\kappa}$ is a physical solution, the corresponding ϕ_κ will have rapidly oscillating wave function between the positive and negative values, and thus becomes a spurious solution. This can be seen in the panels (b), (c), (f), and (g) of Fig. 1. However, half of each envelope of these oscillating wave functions is identical to that of the physical state with the same energy.

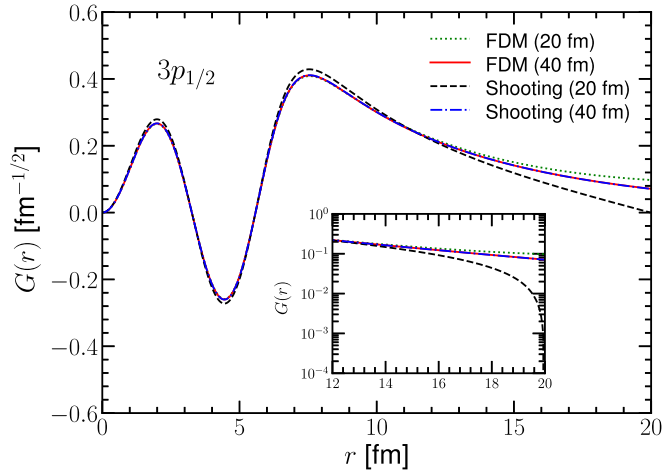

FIG. 2. The wave functions of the large component $G(r)$ of $3p_{1/2}$ state obtained by FDM using 5PADF and the shooting method with box sizes $R_{\rm box} = 20$ fm and 40 fm. The inset shows the asymptotic wave function in logarithmic scale.

One may try to use the five-point CDF that has a higher accuracy to calculate the first-order derivative instead. The obtained results for $\kappa = -1$ and $\kappa = 1$ are listed in columns 5PCDF in Table I. In this case, one can find that the degeneracy between the physical and spurious solutions disappear. This is because there is no longer the unitary matrix U to transform $H_{-\kappa}$ to H_κ. Therefore, the number of spurious states is reduced compared to those obtained by the 3PCDF. This fact was also found in Ref. [7].

To avoid the fermion doubling problem, Ref. [27] used the two-point forward or backward difference formula, i.e., the asymmetric difference formula (ADF), to discretize the Dirac field of the massless fermion in one-dimensional LQCD. Recently, Ref. [31] clearly pointed out in their Fig. 5 that the central symmetric formula (5) uses the wave functions at $r - h$ and $r + h$ to calculate the first-order derivative, but misses the information at r. This can also explain the fact that 5PCDF can produce less spurious states since it misses less information at r comparatively. Therefore, Ref. [31] applied the ADF to calculate the first-order derivative in the mesh-sweeping method to solve the Dirac equation for electrons in two-dimensional graphene.

In the following, we will apply the ADF to calculate the first-order derivative in the FDM to solve the Dirac equation. Taking the three-point formula as an example, the forward or backward difference formulas are

$$\frac{df(r)}{dr} \simeq \frac{-3f(r) + 4f(r+h) - f(r+2h)}{2h},$$
$$\frac{df(r)}{dr} \simeq \frac{f(r-2h) - 4f(r-h) + 3f(r)}{2h}. \qquad (10)$$

One may notice that, if only the forward or backward difference formula was used for both the large and small wave function components, the Dirac Hamiltonian matrix thus established would be non-Hermitian. Actually, we found that, for the wave function components with even parity, the backward difference formula should be applied to guarantee that its derivative is zero at $r = 0$, according to the boundary condition. Instead, for the wave function components with odd parity, the forward difference formula should be used. It should be also noticed that the parities of the large and small components of the same state in the Dirac equation are opposite. Therefore, we should apply the forward or backward difference formula alternatively for the large and small components of the Dirac wave function according to their parities. This prescription can not only guarantee the hermiticity of the Dirac Hamiltonian, but also include the full wave function information while doing the first-order derivatives, and thus eliminate the spurious state.

Explicitly, for the states with $\kappa = -1$, the large (small) component of the Dirac wave function should have odd (even) parity. Then, the upper-right corner matrix $\boldsymbol{B}_1$ in the Dirac Hamiltonian (7) which includes the first-order derivative of the small component should use the backward difference formula. Taking the three-point formula (10) as an example, this matrix can be written as

$$\boldsymbol{B}_{1b} = \begin{pmatrix} \frac{\kappa}{r_1} - \frac{3}{2h} & & & & & \\ \frac{4}{2h} & \frac{\kappa}{r_2} - \frac{3}{2h} & & & & \\ -\frac{1}{2h} & \frac{4}{2h} & \frac{\kappa}{r_3} - \frac{3}{2h} & & & \\ & \ddots & & & & \\ & & -\frac{1}{2h} & \frac{4}{2h} & \frac{\kappa}{r_{n-1}} - \frac{3}{2h} & \\ & & & -\frac{1}{2h} & \frac{4}{2h} & \frac{\kappa}{r_n} - \frac{3}{2h} \end{pmatrix}, \tag{11}$$

and the corresponding matrix $\boldsymbol{B}_2$ at the bottom-left of the Dirac Hamiltonian for the large component should be calculated with the forward difference formula (denoted as $\boldsymbol{B}_{2f}$), which turns out to be the same with $\boldsymbol{B}_{1b}^T$.

The first five bound states obtained by the FDM using the above three-point ADF for the states with $\kappa = -1$ and $\kappa = 1$ are listed in columns 3PADF in Table I. One can find that there is no longer a spurious state. The results have one-to-one correspondence to those obtained by the shooting method. If we use the five-point ADF with higher accuracy, the results listed in columns 5PADF are much closer to those obtained by the shooting method. The largest energy difference appears in the $3p_{1/2}$ state, which is very weakly bound with the energy $E \approx -0.3$ MeV. We have checked that if the box size is enlarged to be $R_{\rm box} = 40$ fm, the 5PADF and shooting method will give the same results -0.292 MeV. Table I shows that with a smaller box, $R_{\rm box} = 20$ fm, the FDM with 5PADF can give more accurate eigenenergy for the weakly bound states than the shooting method.

In Fig. 2, the large components of the wave function for $3p_{1/2}$ obtained by the shooting method and FDM using 5PADF with box sizes $R_{\rm box} = 20$ fm and 40 fm are shown up to $r = 20$ fm. When the box size is $R_{\rm box} = 40$ fm, the wave functions obtained by the two methods are identical. With the box size $R_{\rm box} = 20$ fm, the wave function obtained by the shooting method is obviously different from those obtained with the box size $R_{\rm box} = 40$ fm, especially in the asymptotic region. Comparatively, the wave functions obtained by the FDM with the box $R_{\rm box} = 20$ fm are much closer to those obtained with the box size $R_{\rm box} = 40$ fm. This shows that the FDM is less sensitive to the box size than the shooting method for the weakly bound state. The reason is that the boundary condition for the wave function is $G(r) = 0$ at $r = R_{\rm box}$ in the shooting method, but at $r > R_{\rm box}$ in the FDM.

In summary, the spurious-state problem in the FDM to solve the Dirac equation for massive fermions is resolved directly without any evolution process or adding any other artificial terms. The spurious states are completely eliminated by using the ADF instead of the CDF to calculate the first-order derivative in the Dirac Hamiltonian. To guarantee the hermiticity of the Dirac Hamiltonian, the forward and backward ADFs should be used alternatively for the large and small components of the wave function according to their parities. This prescription is illustrated by the example of neutrons moving in a Dirac Woods-Saxon potential in ^{132}Sn. The feasibility of this prescription is also checked for the hydrogen system. This prescription provides a very simple and efficient technique to apply the FDM for the description of relativistic systems in the fields of atom physics, nuclear physics, particle physics, and so on.

This work was supported in part by the National Natural Science Foundation of China (Grants No. 11775119 and No. 2175109) and the Natural Science Foundation of Tianjin (Grant No. 19JCYBJC30800).

[1] C. J. Horowitz and B. D. Serot, Nucl. Phys. A **368**, 503 (1981).

[2] J. Meng, H. Toki, S. G. Zhou, S. Q. Zhang, W. H. Long, and L. S. Geng, Prog. Part. Nucl. Phys. **57**, 470 (2006).

[3] Y. K. Gambhir, P. Ring, and A. Thimet, Ann. Phys. (NY) **198**, 132 (1990).
[4] S. G. Zhou, J. Meng, and P. Ring, Phys. Rev. C **68**, 034323 (2003).
[5] G. Li-Sheng, J. Meng, and H. Toki, Chin. Phys. Lett. **24**, 1865 (2007).
[6] B. N. Lu, J. Zhao, E. G. Zhao, and S. G. Zhou, Phys. Rev. C **89**, 014323 (2014).
[7] S. Salomonson and P. Öster, Phys. Rev. A **40**, 5548 (1989).
[8] J. Fang, S. Chen, T, Heng, Nucl. Sci. Technol. **31**, 15 (2020).
[9] B. Zhao, Acta Phys. Sin. **65**, 052401 (2016).
[10] C. Bottcher and M. R. Strayer, Ann. Phys. (NY) **175**, 64 (1987).
[11] C. F. Fischer and F. A. Parpia, Phys. Lett. A **179**, 198 (1993).
[12] W. Pöschl, D. Vretenar, and P. Ring, Comput. Phys. Commun. **99**, 128 (1996).
[13] C. Müller, N. Grün, and W. Scheid, Phys. Lett. A **242**, 245 (1998).
[14] S. Zhao, Comput. Methods Appl. Mech. Eng. **196**, 5031 (2007).
[15] H. Almanasreh, S. Salomonson, and N. Svanstedt, J. Comput. Phys. **236**, 426 (2013).
[16] T. T. Sun, L. Qian, C. Chen, P. Ring, and Z. P. Li, Phys. Rev. C **101**, 014321 (2020).
[17] Y. Zhang, H. Liang, and J. Meng, Int. J. Mod. Phys. E **19**, 55 (2010).
[18] K. Hagino and Y. Tanimura, Phys. Rev. C **82**, 057301 (2010).
[19] Y. Tanimura, K. Hagino, and H. Z. Liang, Prog. Theor. Exp. Phys. **2015**, 073D01 (2015).
[20] B. Li, Z. X. Ren, and P. W. Zhao, Phys. Rev. C **102**, 044307 (2020).
[21] P. Ring, Prog. Part. Nucl. Phys. **37**, 193 (1996).
[22] D. Vretenar, A. V. Afanasjev, G. A. Lalazissis, and P. Ring, Phys. Rep. **409**, 101 (2005).
[23] J. Meng and S. G. Zhou, J. Phys. G: Nucl. Part. Phys. **42**, 093101 (2015).
[24] *Relativistic Density Functional for Nuclear Structure*, edited by J. Meng (Word Scientific, Singapore, 2016), Vol. 10.
[25] J. H. Bartlett, Phys. Rev. **88**, 525 (1952).
[26] L. Susskind, Phys. Rev. D **16**, 3031 (1977).
[27] R. Stacey, Phys. Rev. D **26**, 468 (1982).
[28] K. G. Wilson, in *New Phenomena in Subnuclear Physics*, edited by A. Zichichi, The Subnuclear Series Vol. 13 (Springer, New York, 1977), pp. 69–142.
[29] J. B. Kogut, Rev. Mod. Phys. **55**, 775 (1983).
[30] W. Koepf and P. Ring, Z. Phys. A **339**, 81 (1991).
[31] B. Szafran, A. Mreńca-Kolasińska, and D. Żebrowski, Phys. Rev. B **99**, 195406 (2019).